Electronic Supplementary Material (ESI) for Dalton Transactions.
This journal is © The Royal Society of Chemistry 2017

DOTA analogue with phosphinate-iminodiacetate pendant arm: modification of complex formation rate with a strongly chelating pendant

Soňa Procházková, Vojtěch Kubíček,* Zuzana Böhmová, Kateřina Holá, Jan Kotek and Petr Hermann

Department of Inorganic Chemistry, Faculty of Science, Charles University, Hlavova 2030, 128 40 Prague 2, Czech Republic; email: kubicek@natur.cuni.cz; tel.: +420 221951436; fax: +420 22191253

Table of content

Potentiometry - the detailed procedure

Figure S1. ^{1}H, $^{13}C\{^{1}H\}$ and $^{31}P\{^{1}H\}$ NMR spectra of H_6do3aP^{ida}.

Table S1. The experimentally determined overall protonation constants $\log\beta_h$ [a] of H_6do3aP^{ida} and the pre-formed $[Ln(do3aP^{ida})]^{3-}$ complexes.

Table S2. The experimentally determined overall stability constants $\log\beta_{hlm}$ [a] of the H_6do3aP^{ida} complexes.

Table S3. Comparison of the stability constants $\log K_{011}$ [a] of the discussed complexes.

Table S4. The overall stability constants $\log K$ of the ternary complexes with pre-formed $[Gd(do3aP^{ida})]^{3-}$ complex.

Table S5. Comparison of the consecutive stability constants $\log K_{011}$ and $\log K_{021}$ [a] of the ternary complexes of $[Gd(do3aP^{ida})]^{3-}$ with those of the complexes of H_2ida.

Figure S2. ^{31}P NMR titration of H_6do3aP^{ida}.

Figure S3. Distribution diagram of Cu(II)–$[Gd(H_ndo3aP^{ida})]^{n-3}$ system.

Figure S4. Distribution diagram of Eu(III)–$[Gd(H_ndo3aP^{ida})]^{n-3}$ system.

Table S6. Experimental data of the reported crystal structures.

Table S7. The coordination distances found in the crystal structure of $[Cu_4(do3aP^{ida})(OH)(H_2O)_4]Cl\cdot 7.5H_2O$.

Figure S5. The coordination mode of the Cu1 ion in the crystal structure of $[Cu_4(do3aP^{ida})(OH)(H_2O)_4]Cl\cdot 7.5H_2O$.

Figure S6. The coordination mode of the Cu2 ion in the crystal structure of $[Cu_4(do3aP^{ida})(OH)(H_2O)_4]Cl\cdot 7.5H_2O$.

Figure S7. The coordination mode of the Cu3 ion in the crystal structure of $[Cu_4(do3aP^{ida})(OH)(H_2O)_4]Cl\cdot 7.5H_2O$.

Figure S8. The coordination mode of the Cu4 ion in the crystal structure of $[Cu_4(do3aP^{ida})(OH)(H_2O)_4]Cl\cdot 7.5H_2O$.

Figure S9. UV-Vis spectra at the beginning of measurement, corresponding to the *out-of-cage* complex, and at the end of measurement, corresponding to the *in-cage* complex, performed under the 10-fold metal excess.

Figure S10. UV-Vis spectra at the beginning of measurement, corresponding to the *out-of-cage* complex and at the end of measurement, corresponding to the *in-cage* complex, performed under the 10-fold ligand excess.

Figure S11. Changes of absorption spectra in the course of complexation and time dependences of absorbance at 314 nm.

Potentiometry - the detailed procedure

The stock solution of hydrochloric acid (~0.03 M) was prepared from 35 % aqueous solution (puriss, Fluka). Commercial $(NMe_4)Cl$ (99 %, Fluka) was recrystallized from boiling *i*-PrOH and the solid salt was dried over P_2O_5 in vacuum to constant weight (this dried form of the salt is extremely hygroscopic). Carbonate-free $(NMe_4)OH$ solution (~0.2 M) was prepared from $(NMe_4)Cl$ using ion exchanger Dowex 1 in the OH^--form (elution with carbonate-free water, under argon). The hydroxide solution was standardized against potassium hydrogen phthalate and the HCl solution against the ca. 0.2 M $(NMe_4)OH$ solution. Stock solutions of the individual metal cations were prepared by dissolving hydrates of metal chlorides and the metal ions contents were determined by titration with a standard Na_2H_2edta solution. Analytical concentration of a stock solution of the ligand was determined together with refinement of protonation constants using OPIUM software package (see below). The in-cell titrations were carried out in a vessel thermostatted at 25.0 ± 0.1 °C, at ionic strength I = 0.1 M ($(NMe_4)Cl$; with pK_w = 13.81) and in the presence of extra HCl using a PHM 240 pH-meter, a 2-ml ABU 900 automatic piston burette and a GK 2401B combined electrode (all Radiometer, Denmark). The in-cell titrations were carried out in pH range 1.7–12.0 with at least 40 points per titration and four parallel titrations (c_L = 0.004 M, c_M = 0.004 M or 0.002 M or 0.008 M).

The stability constants of the Ln(III) complexes were obtained by the out-of-cell method. The batches (starting volume 1 ml) were prepared under Ar stream in tubes with ground joints from ligand, metal ion and HCl/$(NMe_4)Cl$ stock solutions and water ($c_L = c_M$ ~ 0.004 M, 5% ligand excess). Then a known amount of $(NMe_4)OH$ standard solution was added under Ar. The tubes were firmly closed with stoppers and the solutions were equilibrated at room temperature for 4 weeks (one batch was checked after 6 weeks and gave the same data). Titrations were performed in the pH ranges 1.5–3.8 (final pH values) with around 20 data points per whole titration and three titrations per system.

The pre-formed Ln(III) complexes in solution were obtained by mixing of the ligand stock solution (5 % molar excess) with Ln(III) ion stock solution in a glass ampoule and a slow portion-wise addition (2 h) of standard $(NMe_4)OH$ solution (just to neutralize the ligand amount) under Ar. The ampoule was flame-sealed and left at 80 °C overnight to fully complex the metal ion. The ampoules were opened under Ar and aliquots of the solutions of the Ln(III) complexes were transferred into a titration vessel. Water and excess of HCl, metal ion stock solution and $(NMe_4)Cl$ solutions were added (to reach a pH of about 1.8 and I = 0.1 M $(NMe_4)Cl$ in the final solution, starting volume 5 ml, the preformed complex concentration ~0.004 M) and the solution was immediately titrated with a standard $(NMe_4)OH$ solution at 25.0 °C acquiring at least 40 data points per each of three titrations.

The constants (with standard deviations) were calculated with program OPIUM.[1] The program minimizes the criterion of the generalized least-squares method using the calibration function

$$E = E_0 + S \times \log[H^+] + j_1 \times [H^+] + j_2 \times K_w / [H^+]$$

where the additive term E_0 contains the standard potentials of the electrodes used and contributions of inert ions to the liquid-junction potential, S corresponds to the Nernstian slope, the value of which should be close to the theoretical value and the j_1[H+] and $j_2[OH^-]$ terms are the contributions of the H^+ and OH^- ions to the liquid-junction potential. The calibration parameters were determined from titration of standard HCl with standard $(NMe_4)OH$ before and after

[1] Kývala, M.; Lukeš, I. *International Conference, Chemometrics '95*; Pardubice, Czech Republic, 1995; p 63; full version of *"OPIUM"* is available (free of charge) on http://www.natur.cuni.cz/~kyvala/opium.html.

each ligand or ligand–metal titration to give pairs of calibration/titration, which was used for calculations of the constants. The overall protonation constants β_n are concentration constants, defined by $\beta_n = [H_nL]/([H]_n[L])$ (they were transformed to dissociation constants as $pK_1 = \log\beta_1$ and $pK_n = \log\beta_n - \log\beta_{n-1}$). The (concentration) stability constant are defined by $\beta_{hlm} = [H_hL_lM_m]/([H]^h[L]^l[M]^m)$.

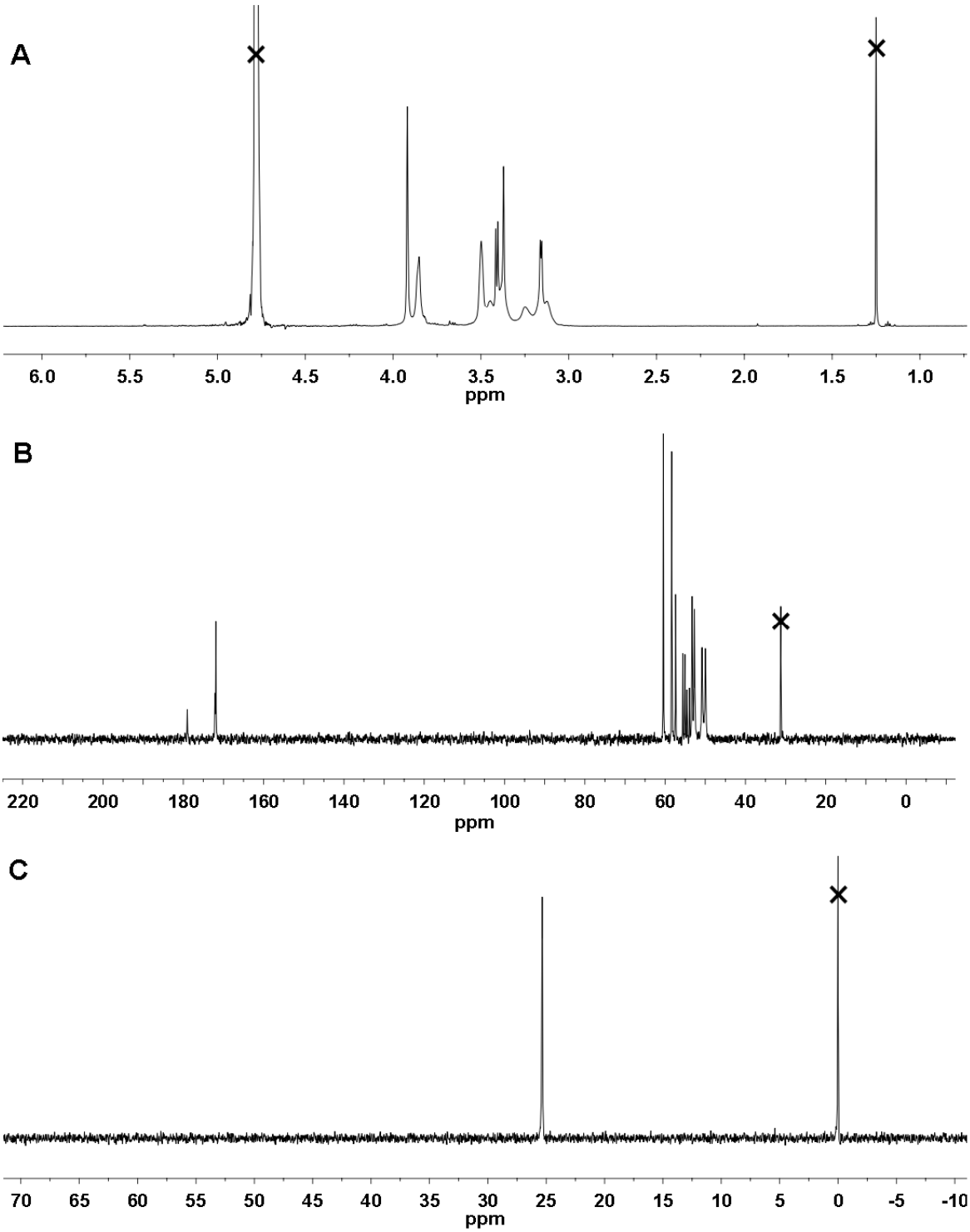

Figure S1. ^{1}H (A), $^{13}C\{^{1}H\}$ (B) and $^{31}P\{^{1}H\}$ (C) NMR spectra of H_6do3aP^{ida} (25 °C, pD = 6). Signals of solvent and standards are labeled with crosses.

Table S1. The experimentally determined overall protonation constants $\log\beta_h$[a] of H_6do3aP^{ida} and the pre-formed $[Ln(do3aP^{ida})]^{3-}$ complexes (25 °C, I = 0.1 M $(NMe_4)Cl$).

h	H_6do3aP^{ida}	$[La(do3aP^{ida})]^{3-}$	$[Nd(do3aP^{ida})]^{3-}$	$[Eu(do3aP^{ida})]^{3-}$	$[Gd(do3aP^{ida})]^{3-}$	$[Y(do3aP^{ida})]^{3-}$
1	12.85(4)	7.67(2)	7.83(3)	7.83(1)	7.79(2)	7.95(1)
2	22.48(4)	10.25(3)	10.29(4)	10.23(1)	10.53(2)	10.52(1)
3	30.61(4)	11.88(3)	11.80(4)	11.82(1)	12.09(2)	12.29(1)
4	35.01(4)	–	–	–	–	–
5	38.28(4)	–	–	–	–	–
6	40.26(5)	–	–	–	–	–
7	41.85(5)	–	–	–	–	–

[a] For the free ligand, $\beta_h = [H_hL] / ([H]^h \times [L])$. For the pre-formed complexes, $\beta_h = [H_h(ML)] / ([H]^h \times [ML])$.

Table S2. The experimentally determined overall stability constants $\log\beta_{hlm}$[a] of the H_6do3aP^{ida} complexes (25 °C, I = 0.1 M $(NMe_4)Cl$).

Species[b]	Cu(II)	Zn(II)	La(III)	Nd(III)	Eu(III)	Gd(III)	Y(III)
[M(L)]	23.75(3)	21.79(2)	22.09[c]	24.02[c]	24.94[c]	25.27[c]	25.39[c]
[M(HL)]	32.15(2)	30.25(1)	29.76(3)	31.85(3)	32.77(3)	33.06(9)	33.34(5)
$[M(H_2L)]$	35.99(2)	34.01(2)	32.96(5)	34.79(2)	35.72(2)	35.66(9)	35.74(7)
$[M(H_3L)]$	–	36.99(1)	36.19(2)	37.01(3)	37.99(3)	37.79(11)	37.94(7)
$[M_2(L)]$	34.71(3)	31.37(1)	[d]	[d]	[d]	[d]	[d]
$[M_2(HL)]$	38.71(2)	35.05(1)	[d]	[d]	[d]	[d]	[d]
$[M_2(H_2L)]$	40.30(3)	–	[d]	[d]	[d]	[d]	[d]
$[M_2(L)(OH)]$	25.51(3)	21.20(2)	[d]	[d]	[d]	[d]	[d]
$[M_2(L)(OH)_2]$	13.46(4)	–	[d]	[d]	[d]	[d]	[d]

[a] $\beta_{hlm} = [H_hL_lM_m] / ([H]^h \times [L]^l \times [M]^m)$. [b] Charges are omitted for clarity reasons. [c] Calculated using the protonation constants determined for the pre-formed complexes. [d] The systems were studied by out-of-cell method and, thus, only in 1:1 metal-to-ligand ratio was utilized.

Table S3. Comparison of the stability constants logK_{011}[a] of the discussed complexes.

Ligand	Cu(II)	Zn(II)	La(III)	Nd(III)	Eu(III)	Gd(III)	Y(III)
H_4dota [2]	22.3	20.8	22.0	23.7	23.0	24.0	24.0
H_6do3aP^{ida}	23.75	21.79	22.09	24.02	24.94	25.27	25.39
H_5do3aP^{PrA} [3]	–	–	23.1	–	25.3	25.04	24.63

[a] K_{011} = [M(L)] / ([L] × [M]).

Table S4. The overall stability constants log$K$ of the ternary complexes with pre-formed [Gd(do3aP^{ida})]$^{3-}$ complex (25 °C, I = 0.1 M (NMe_4)Cl).

Equilibrium[a]	Cu(II)	Zn(II)	Ca(II)	Eu(III)
M + {Gd(L)} = [M{Gd(L)}]	10.53(1)	8.10(3)	5.19(5)	8.98(2)
M + {Gd(L)} + H^+ = [M{Gd(HL)}]	–	–	–	11.57(3)
M + {Gd(L)} + H_2O = [M{Gd(L)}(OH)] + H^+	1.47(3)	–	–6.69(5)	–
M + {Gd(L)} + 2H_2O = [M{Gd(L)}$(OH)_2$] + 2H^+	–10.15(4)	–	–	–
M + 2{Gd(L)} = [M{Gd(L)}$_2$]	15.40(7)	13.30(7)	–	16.31(8)
M + 2{Gd(L)} + H^+ = [M{Gd(HL)}{Gd(L)}]	20.95(4)	18.47(8)	–	20.61(2)
M + 2{Gd(L)} + H_2O = [M{Gd(L)}$_2$(OH)] + H^+	5.39(7)	2.59(9)	–	6.0(1)
M + 2{Gd(L)} + 2H_2O = [M{Gd(L)}$_2$$(OH)_2$] + 2$H^+$	–	–	–	–6.4(1)

[a] Charges are omitted for clarity reasons.

Table S5. Comparison of the consecutive stability constants logK_{011} and logK_{021}[a] of the ternary complexes of [Gd(do3aP^{ida})]$^{3-}$ with those of the complexes of H_2ida.[2]

Species[b]	Cu^{2+}		Zn^{2+}		Ca^{2+}		Eu^{3+}	
	[Gd(do3aP^{ida})]	H_2ida	[Gd(do3aP^{ida})]	H_2ida	[Gd(do3aP^{ida})]	H_2ida	[Gd(do3aP^{ida})]	H_2ida
[M(X)]	10.53	10.6	8.10	7.03	5.19	2.59	8.98	6.2
[M$(X)_2$]	4.87	5.7	5.20	5.4	–	–	7.33	4.5

[a] K_{011} = [M(X)] / ([X] × [M]) and K_{021} = [M$(X)_2$] / ([X] × [M(X)]), where X = [Gd(do3aP^{ida})]$^{3-}$ or X = ida^{2-}. [b] Charges are omitted for clarity reasons.

[2] A. E. Martell, R. M. Smith, *Critical Stability Constants*, Plenum Press, New York, 1974–1989, vol. 1–6; *NIST Standard Reference Database 46 (Critically Selected Stability Constants of Metal Complexes)*, version 5.0, 1994.

[3] M. Försterová, I. Svobodová, P. Lubal, P. Táborský, J. Kotek, P. Hermann, I. Lukeš *Dalton Trans.*, 2007, 535–549.

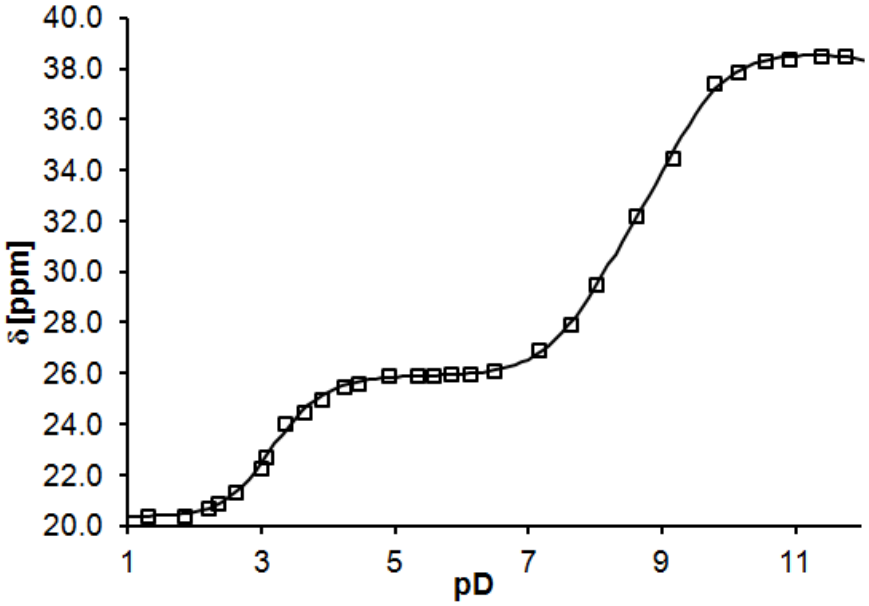

Figure S2. ^{31}P NMR titration of H_6do3aP^{ida}.

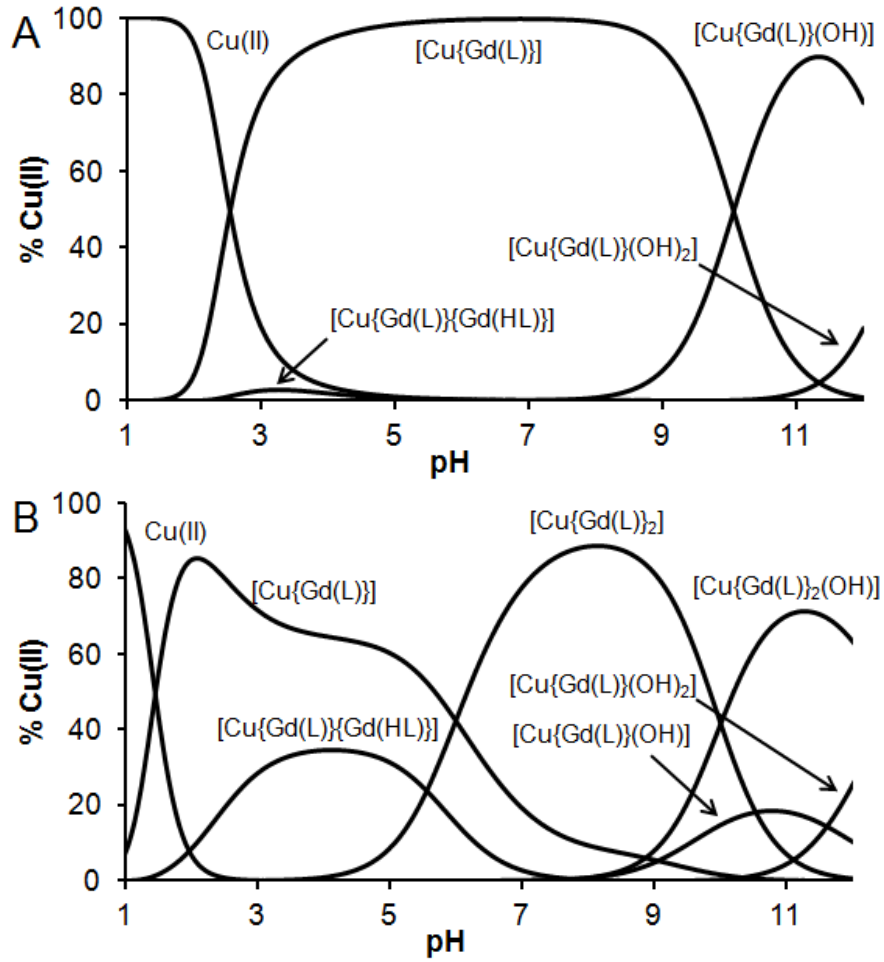

Figure S3. Distribution diagram of Cu(II)–[Gd($H_n$do3aP^{ida})]$^{n-3}$ system (25 °C, I = 0.1 M $(NMe_4)Cl$, c_{GdL} = 4 mM , c_M = 4 mM (**A**) c_M = 2 mM (**B**)). Charges are omitted for clarity reasons.

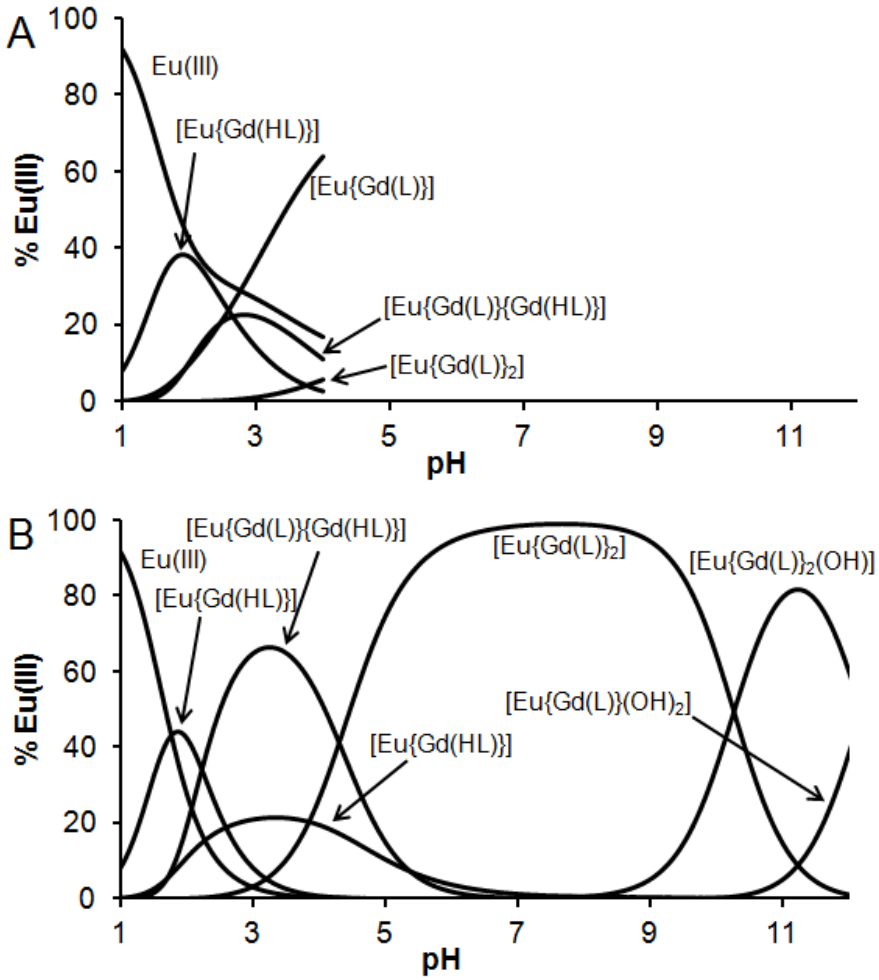

Figure S4. Distribution diagram of Eu(III)–[Gd($H_n$do3aP^{ida})]$^{n-3}$ system (25 °C, I = 0.1 M (NMe_4)Cl, c_{GdL} = 4 mM, c_M = 4 mM (**A**) c_M = 2 mM (**B**)). Charges are omitted for clarity reasons.

Table S6. Experimental data of the reported crystal structures.

Compound	H_6do3aP^{ida}·4H_2O	[Cu_4(do3aP^{ida})(OH)(H_2O)$_4$]Cl·7.5H_2O
Formula	$C_{20}H_{36}N_5O_{12}P$·4H_2O	$C_{20}H_{39}Cu_4N_5O_{17}PCl$·7.5$H_2O$
M_r	641.57	1077.26
Colour	colorless	blue
Shape	prism	prism
Dimensions (mm)	0.35×0.13×0.10	0.30×0.25×0.21
Crystal system	triclinic	triclinic
Space group	P_{-1}	P_{-1}
a (Å)	9.5462(4)	12.0847(5)
b (Å)	10.7017(7)	12.4493(5)
c (Å)	16.0510(10)	12.9847(5)
α (°)	100.877(2)	85.606(2)
β (°)	95.356(4)	78.603(2)
γ (°)	112.760(3)	86.931(2)
V (Å^3)	1459.66(15)	1907.87(13)
Z	2	2
D_c (g·cm^{-3})	1.460	1.875
μ (mm^{-1})	0.176	2.407
F(000)	684	1106
Reflections unique; observed ($I_o > 2\sigma(I)$)	5679; 3638	7764; 8790
Parameters	388	523
G-o-f on F^2	1.057	1.125
R; R' (all data)	0.0728; 0.1119	0.0404; 0.0489
wR; wR' (all data)	0.2071; 0.2370	0.0977; 0.1042
Difference max; min (e Å^{-3})	1.329; 0.474	1.675; 1.146

Table S7. The coordination distances found in the crystal structure of [Cu_4(do3aP^{ida})(OH)(H_2O)$_4$]Cl·7.5H_2O.

Bond	Distance [Å]	Bond	Distance [Å]
Cu1–N1	2.066(3)	Cu2–O241	1.946(3)
Cu1–N4	2.101(3)	Cu2–O261	1.951(3)
Cu1–N7	2.059(3)	Cu2–N22	2.018(3)
Cu1–N10	2.089(3)	Cu2–O412[a]	1.930(3)
Cu1–O311	2.489(2)	Cu2–O1C	2.497(4)
Cu1–O511	2.216(3)	Cu2–O11	2.697(3)
Bond	Distance [Å]	Bond	Distance [Å]
Cu3–O11	1.927(2)	Cu4–O512[a]	1.919(3)
Cu3–O311	1.972(2)	Cu4–O312	1.939(3)
Cu3–O2C	1.977(2)	Cu4–O5C	2.005(3)
Cu3–O2C[b]	1.976(2)	Cu4–O2C[b]	2.042(2)
Cu3–O511	2.376(2)	Cu4–O3C	2.268(3)
Cu3–O3C	2.491(3)	Cu4–O4C	2.412(3)

[a] Symmetrically-associated ligand molecule. [b] Symmetrically-associated hydroxido ligand.

Figure S5. The coordination mode of the Cu1 ion in the crystal structure of $[Cu_4(do3aP^{ida})(OH)(H_2O)_4]Cl\cdot 7.5H_2O$. The hydrogen atoms attached to the carbon atoms are not displayed for the clarity reasons.

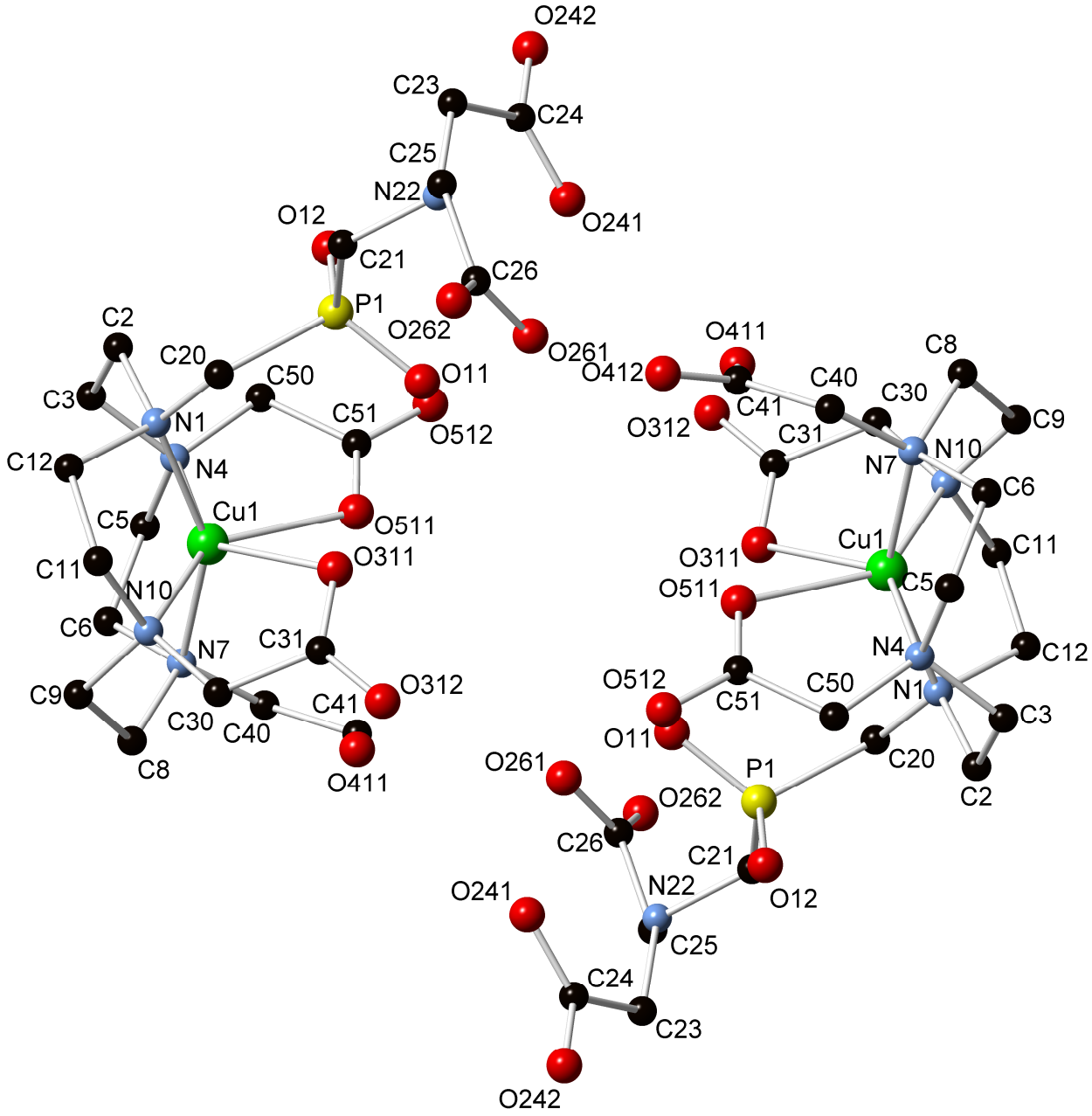

Figure S6. The coordination mode of the Cu2 ion in the crystal structure of $[Cu_4(do3aP^{ida})(OH)(H_2O)_4]Cl{\cdot}7.5H_2O$. The hydrogen atoms attached to the carbon atoms are not displayed for the clarity reasons.

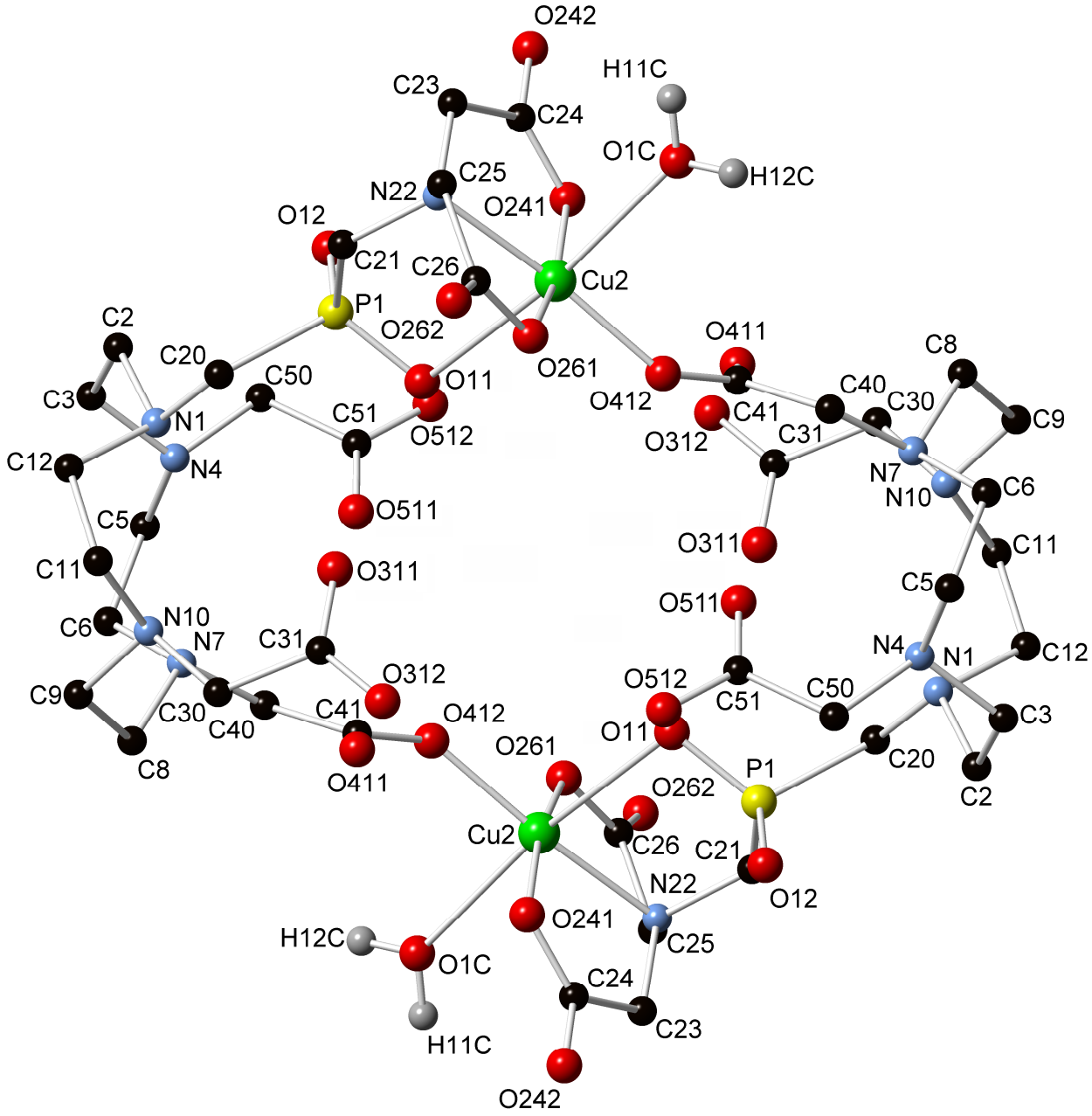

Figure S7. The coordination mode of the Cu3 ion in the crystal structure of $[Cu_4(do3aP^{ida})(OH)(H_2O)_4]Cl{\cdot}7.5H_2O$. The hydrogen atoms attached to the carbon atoms are not displayed for the clarity reasons.

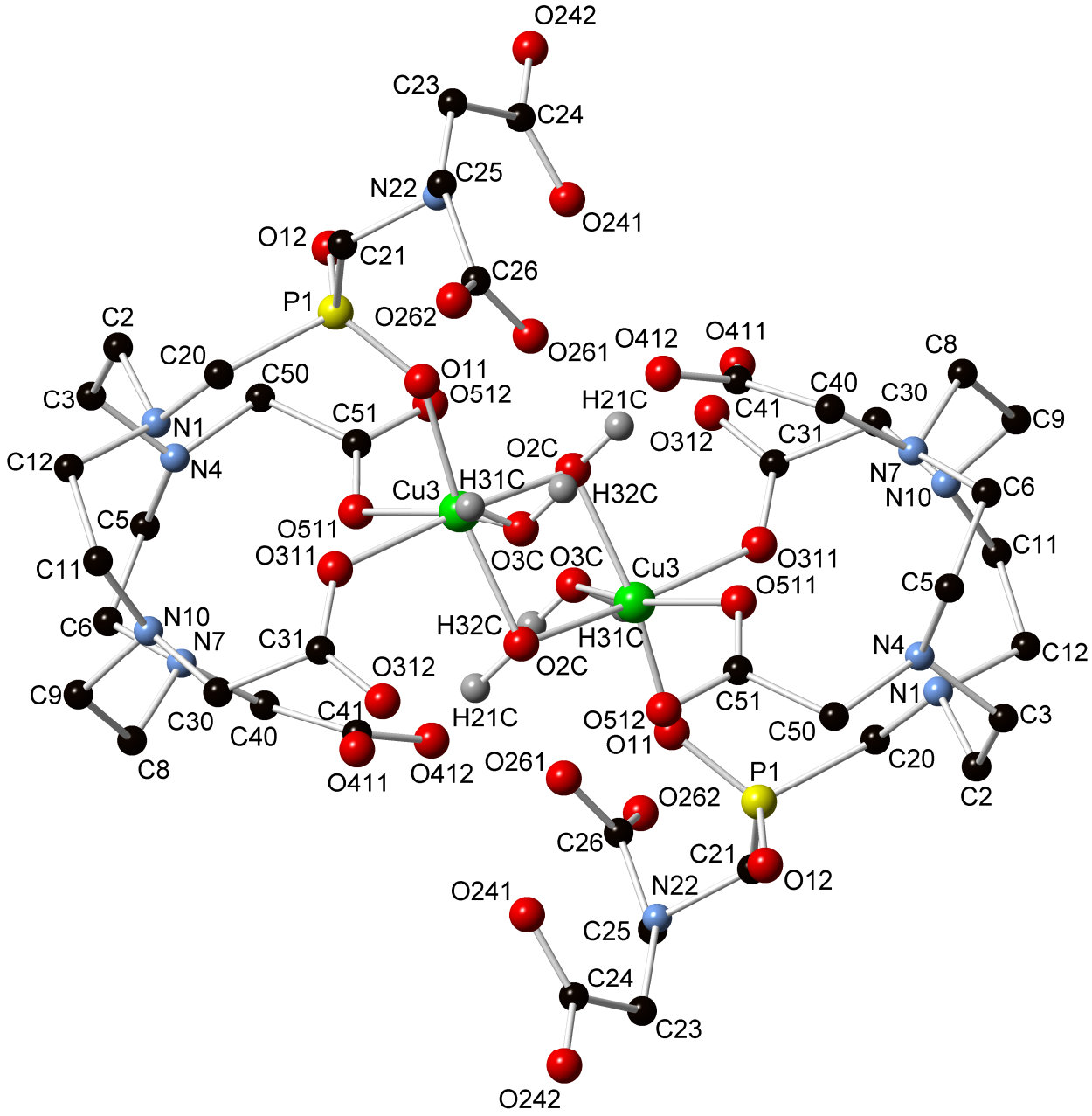

Figure S8. The coordination mode of the Cu4 ion in the crystal structure of $[Cu_4(do3aP^{ida})(OH)(H_2O)_4]Cl{\cdot}7.5H_2O$. The hydrogen atoms attached to the carbon atoms are not displayed for the clarity reasons.

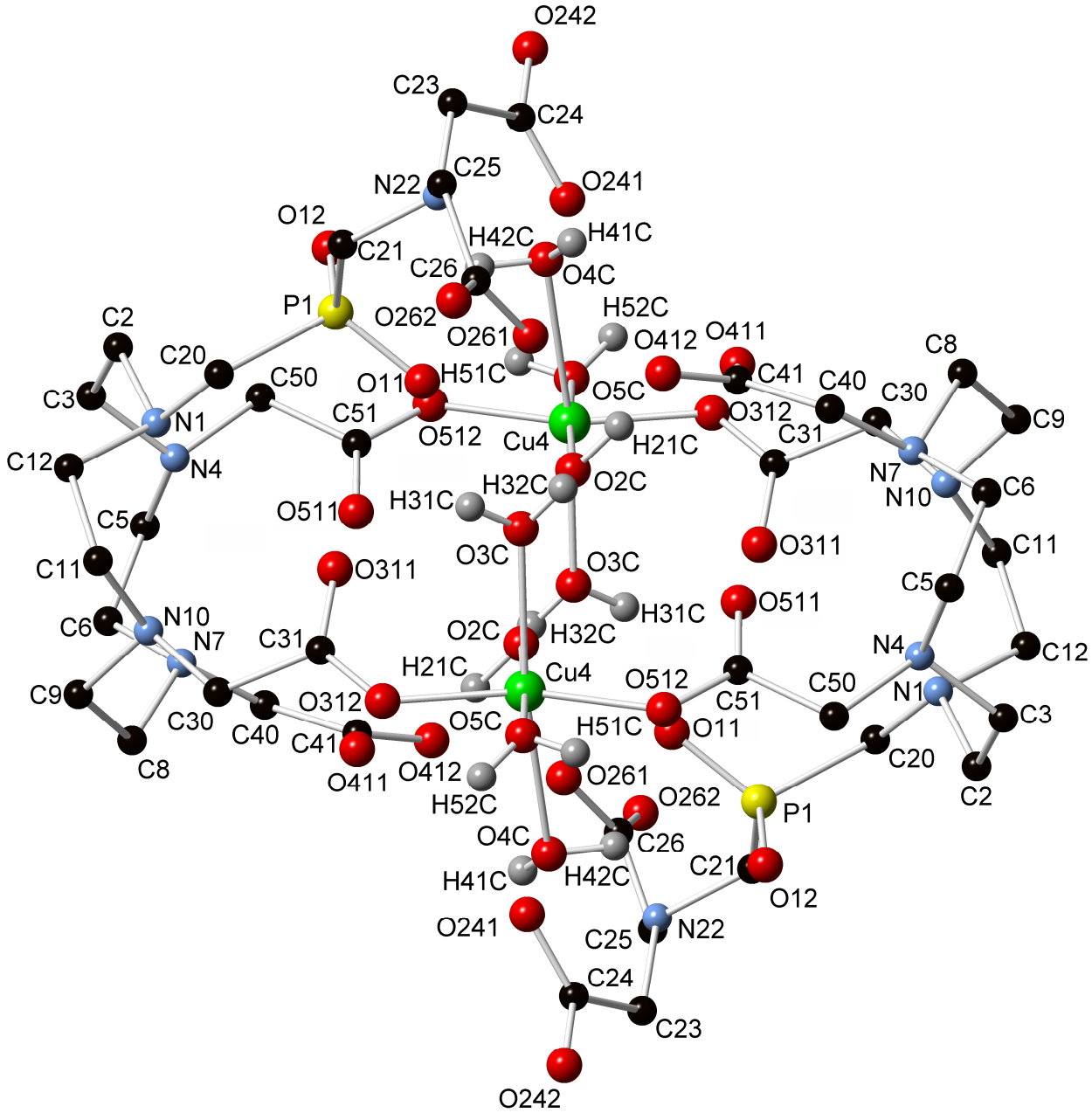

Figure S9. UV-Vis spectra at the beginning of measurement, corresponding to the *out-of-cage* complex (blue), and at the end of measurement, corresponding to the *in-cage* complex (red), performed under the 10-fold metal excess (pH = 6.5, $c_{Ce} = 5.0 \cdot 10^{-3}$ M, $c_L = 5.0 \cdot 10^{-4}$ M, 25 °C). The increasing absorbance at short wavelengths results from the Ce(III) ion excess. Similar spectra were observed along the whole studied pH range.

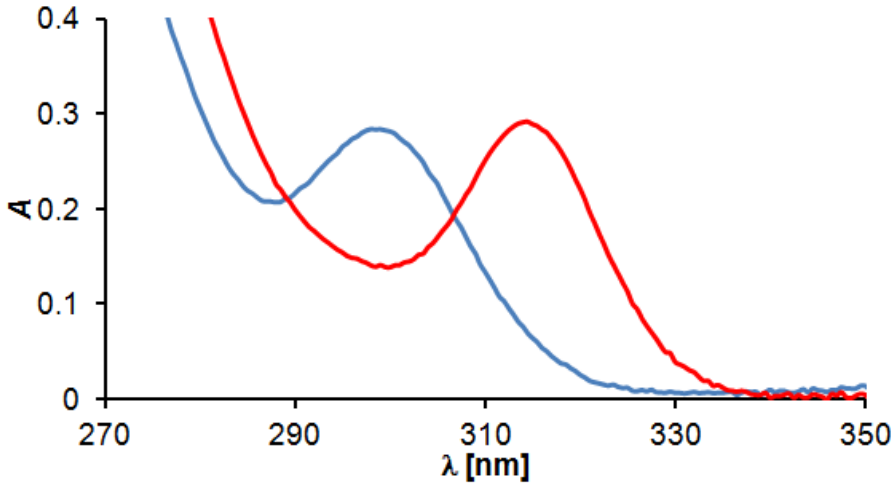

Figure S10. UV-Vis spectra at the beginning of measurement, corresponding to the *out-of-cage* complex (**A**, the spectra change with pH), and at the end of measurement, corresponding to the *in-cage* complex (**B**, pH = 6.5, similar spectra were observed along the whole studied pH range), performed under the 10-fold ligand excess ($c_{Ce} = 5.0 \cdot 10^{-4}$ M, $c_L = 5.0 \cdot 10^{-3}$ M, 25 °C).

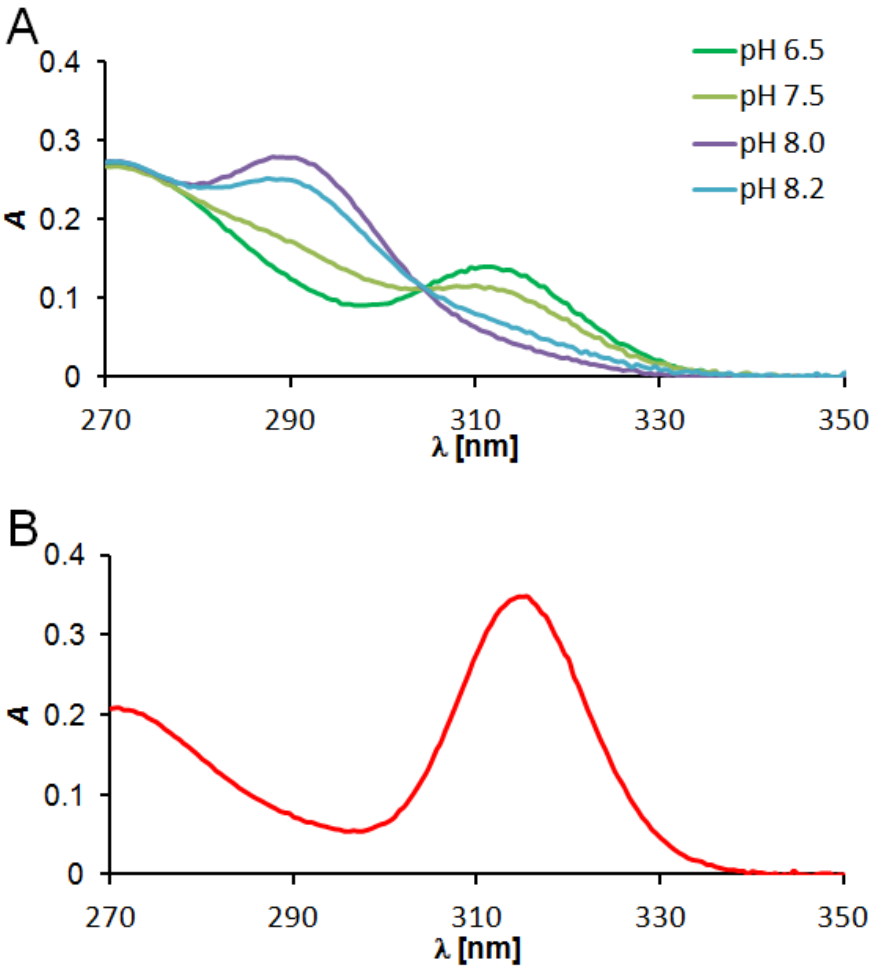

Figure S11. Changes of absorption spectra in the course of complexation (left, pH = 6, 25 °C) and time dependences of absorbance at 314 nm (right). The curves represent the best fit according to Equation 1. **A**: $c_{Ce} = 5.0 \cdot 10^{-4}$ M, $c_L = 5.0 \cdot 10^{-4}$ M; **B**: $c_{Ce} = 5.0 \cdot 10^{-4}$ M, $c_L = 5.0 \cdot 10^{-3}$ M; **C**: $c_{Ce} = 5.0 \cdot 10^{-3}$ M, $c_L = 5.0 \cdot 10^{-4}$ M.